

See discussions, stats, and author profiles for this publication at: <https://www.researchgate.net/publication/303406636>

# Mechanical characterization and thermal conductivity measurements using a new ‘small hot-box’ apparatus: innovative insulating reinforced coatings analysis

Article in Journal of Building Engineering · May 2016

DOI: 10.1016/j.jobe.2016.05.005

---

CITATIONS

13

6 authors, including:



C. Buratti

Università degli Studi di Perugia

139 PUBLICATIONS 2,313 CITATIONS

[SEE PROFILE](#)

---

READS

181



Elisa Belloni

Università degli Studi di Perugia

46 PUBLICATIONS 586 CITATIONS

[SEE PROFILE](#)



Leandro Lunghi

Università degli Studi di Perugia

4 PUBLICATIONS 32 CITATIONS

[SEE PROFILE](#)



Antonio Borri

Università degli Studi di Perugia

208 PUBLICATIONS 2,653 CITATIONS

[SEE PROFILE](#)

Some of the authors of this publication are also working on these related projects:



F-EIR Conference 2021 — Environment Concerns and its Remediation [View project](#)



Seismic assessment of monumental building [View project](#)



# Mechanical characterization and thermal conductivity measurements using a new 'small hot-box' apparatus: innovative insulating reinforced coatings analysis



C. Buratti <sup>a,\*</sup>, E. Belloni <sup>a</sup>, L. Lunghi <sup>a</sup>, A. Borri <sup>a</sup>, G. Castori <sup>a</sup>, M. Corradi <sup>a,b</sup>

<sup>a</sup> Department of Engineering – University of Perugia, Via Duranti 67, 06125 Perugia, Italy

<sup>b</sup> Mechanical and Construction Engineering Department, Northumbria University, Wynne-Jones Building, NE1 8ST Newcastle upon Tyne, United Kingdom

## ARTICLE INFO

### Article history:

Received 20 August 2015

Received in revised form

19 December 2015

Accepted 20 May 2016

Available online 21 May 2016

### Keywords:

Reinforced insulated coatings

Mechanical resistance

Thermal conductivity

Innovative experimental apparatus

## ABSTRACT

The insulation of the building envelope contributes to the reduction of annual energy consumptions. The development of new materials, such as fibre reinforced insulating coatings, could be useful in order to obtain an effective solution for the improvement of energy performance and for reinforcement of the walls.

The evaluation of the thermal and mechanical characteristics of building coatings with good thermal insulation properties and mechanical resistance is the aim of the present paper. A new experimental apparatus, Small Hot-Box, built at the University of Perugia, was used for the evaluation of the thermal conductivity of four different coatings (with and without a reinforced structure). No European standards are available for this innovative facility, but it takes into account some prescriptions of EN ISO 8990. The apparatus was calibrated with materials of known thermal conductivity. The thermal conductivity can be calculated with both the thermal flux meter and the Hot Box method. Good values of the thermal conductivity, in the range of 0.09–0.11 W/mK were found for all the samples, except for one (0.21–0.24 W/mK).

Mechanical tests were also carried out in laboratory on all the samples and results were used to evaluate the shear modulus and strength of the wall panels.

© 2016 Elsevier Ltd. All rights reserved.

## 1. Introduction

Energy consumption for buildings heating and air conditioning represents on average 40% of energy consumptions in Europe [1]. Furthermore a relevant part of the building heritage in Europe is constituted by old buildings [2–4] with poor quality insulation materials. Therefore, recent regulations, as for example the EU Directive 2010/31 [5] on energy efficiency in buildings, aims at increasing target energy efficiency standards, considering both the single components and the entire building. The building envelope plays a fundamental role in energy balance. The evaluation of the building components thermal properties requires a high level of accuracy and many experimental methods for the thermal characterization of materials have been performed from research efforts all over the world. Several methods for measuring the thermal properties are well known; the guarded hot plate is the most common method used for the evaluation of the thermal conductivity of an homogeneous or multilayer material [6]. Many studies concerning the characterization of thermal properties of materials are available; André et al. [7] presented an experimental

set-up based on the hot wire method for the thermal characterization of materials, while a tiny hot plate method is proposed by Jannot et al. [8,9] for the thermal conductivity measurement of heterogeneous materials [10].

Furthermore, for non-homogeneous structures, composed by different materials or components (such as doors, windows or French windows), or when the heat transfer is two - or three-dimensional, different techniques are used; the most common method for the thermal transmittance evaluation is the calibrated Hot-Box [11,12]. Since the seventies the guidelines for Hot Box design criteria are reported in EN ISO 8990 [13] and EN ISO 12567-1 [14]. In particular EN ISO 12567-1 specifies a method to measure the thermal transmittance of doors or windows, but also the thermal conductivity of homogeneous materials can be evaluated. The heat flux through the sample can be evaluated using thermal flux meters installed on the surface of the sample (Thermal Flux Meter Method, TFM). In this case the thermal conductivity of the panel will be calculated as the ratio between the thermal flux and the surface. The flux meter methodology is also considered in the UNI EN 1934:2000 [15]. At the University of Perugia (Department of Engineering), a Calibrated Hot Box was built in 2008, according to UNI EN ISO 8990 [13,16]. It is composed of two chambers (dimensions 2.5 × 1.2 × 3.2 m height), the cold and the hot one [16–20].

\* Corresponding author.

E-mail address: [cinzia.buratti@unipg.it](mailto:cinzia.buratti@unipg.it) (C. Buratti).

<b>Nomenclature</b>	
$A$	panel surface ( $\text{m}^2$ )
$e$	error (%)
$f_t$	tensile strength (MPa)
$G$	shear modulus (MPa)
$\lambda$	thermal conductivity (W/mK)
$P$	power (W)
$p$	diagonal compression load (kN)
$q$	heat flux (W/ $\text{m}^2$ )
$R_t$	thermal resistance ( $\text{m}^2\text{K}/\text{W}$ )
$s$	thickness (m)
$T$	temperature ( $^\circ\text{C}$ )
<i>Subscripts</i>	
$a$	air
$C$	Cold side

Considering homogeneous materials, other experimental apparatus could be used: the guarded hot plate or heat flow meter method (EN ISO 12667 and ASTM C518-10 [21,22]). The heat flow meter apparatus is a comparative device and requires a reference material with known thermal properties for calibration. The heat flow meter apparatus establishes steady state one-dimensional heat flux through a test specimen between two parallel plates at constant but different temperatures [23].

In this context, in the present study measurements with a new experimental apparatus, named Small Hot-Box, were carried out. The experimental system has been designed and built at the Laboratory of Thermal Science, University of Perugia. The apparatus allows the evaluation of the thermal conductivity of homogeneous materials, but the operating principle arises from the Hot-Box method. The advantage of the apparatus with respect to Hot-Box is the possibility of testing homogeneous materials with smaller samples ( $300 \times 300 \text{ mm}$ ); with respect to the Hot Plate apparatus, it can provide a thermal transmittance value measured in conditions similar to the in-situ ones.

Fibre reinforced insulating coatings were characterized with the innovative apparatus. The mechanical properties of the same samples were also evaluated, in order to show the influence of the fibres on the mechanical resistance.

Retrofitting techniques for masonry constructions are extensively found in the existing literature. FRP (Fibre-Reinforced Polymer) systems are increasingly used to strengthen masonry structures: reinforcement is frequently bonded to the surface of existing walls, where it provides tensile strength and prevents the opening of cracks [24–27].

The use of FRPs without epoxy adhesives is less well established [28,29]. Only recently the use of non-organic matrixes has been the subject of research, and it could be a valid alternative to the use of epoxy matrixes. Mechanical tests were conducted in laboratory on  $1.2 \times 1.2 \times 0.24 \text{ m}$  brickwork panels. All wall panels were subjected to shear strength and test results were used to evaluate the shear strength of the masonry before and after the application of the strengthening made of a G-FRP (Glass Fibre-Reinforced Polymer) reinforced insulation coating applied on both panel sides.

Insulation coatings can be used in many applications, such as refurbishment of old buildings, on internal as well as external surfaces, and they should offer a non-invasive method for reinforce historic buildings and saving energy without altering their forms. Fibre-Reinforced Polymers (FRP) are composed of high-strength fibres (such as glass) embedded in a polymer resin (such as

$f$	fans
$H$	Hot side
$HB$	Hot Box method
$i$	input
$m$	mean
$p$	panel
$r$	resistance of the hot side
$s$	specimen
$S$	surface
$tfm$	thermal flux meter method
$w$	walls

polyester), durable (thanks to the resin), and lightweight. Glass fibre reinforced concrete is a composite material made of components with different mechanical properties: cement mortar and G-FRP in place of metal grids. Cement avoids buckling of glass fibres when compressing them, glass fibres improve the tensile strength and ductility. This solution is very diffused in order to improve the shearing strength of the walls [30,31]. Thermal insulation plasters, as the samples investigated in the present study, consisting in innovative reinforced coatings made of mortar and G-FRP, try to combine good mechanical and thermal properties for building refurbishment. Innovative coating solutions are therefore in development, such as aerogel-based high performance insulating plasters, but a limited number of studies exists in this field, probably due to the high costs of the innovative system [32,33].

## 2. Materials and methods

### 2.1. Description of the samples

Four mortars with different chemical compositions were investigated, each one with and without G-FRP, for eight samples in total. The G-FRP grid is characterized by a 66 mm square mesh inserted into the matrix. It is produced by Fibre Net (Udine, Italy)

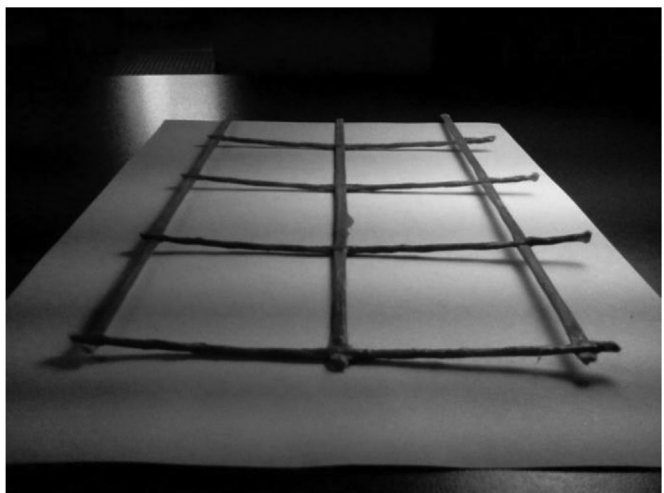


Fig. 1. G-FRP grid.

**Table 1**  
GFRP mesh mechanical properties.

<b>Horizontal direction</b>	Tensile strength (MPa)	530
	Sample size	10
	Cross section (mm <sup>2</sup> )	7.29
	Elongation at failure (%)	1.73
	Young modulus (GPa)	36.1
<b>Vertical direction</b>	Tensile strength (MPa)	680
	Sample size	10
	Cross section (mm <sup>2</sup> )	9.41
	Elongation at failure (%)	1.93
	Young modulus (GPa)	39.8
<b>Weight density</b>	(kg/m <sup>2</sup> )	0.5

and is fabricated with an AR (Alkali Resistant) fibre glass (Fig. 1 and Table 1).

Samples for thermal measurements were made by using a layer of plasterboard as support base. Nine square samples were therefore realized, (including a plasterboard (PL), 13 mm thickness, without coating), with external dimensions 0.3 × 0.3 m (total area of 0.09 m<sup>2</sup>), according to the dimensions of the opening for the sample placement. The thickness of the specimens and the description of the coatings for thermal measurements are reported in Table 2.

Cylindrical samples approximately 94 mm in diameter and approximately 180 mm in height were produced for compression tests; 10 square walls 1.2 m × 1.2 m were assembled in laboratory for shear tests.

## 2.2. Thermal characterization

The new experimental apparatus was built at the Laboratory of Thermal Science – the University of Perugia – for thermal conductivity measurements [34]. A general view of the apparatus is represented in Fig. 2. It is composed of one box (external dimensions 0.94 × 0.94 × 0.50 m) that behaves as hot chamber: the outer walls of the chamber are made of very thick insulation (200 mm of foam polyurethane + 20 mm of wood), in order to minimize the thermal losses and the heat flux through the walls. The thermal conductivity  $\lambda$  of the expanded polyurethane is 0.0245 W/m K and the thermal transmittance of the walls is 0.114 W/m<sup>2</sup>K. The second part of the experimental system is the closure side of the box (dimensions 0.94 × 0.94 × 0.20 m thick): it is a sandwich wall composed of two panels of wood (20 mm each) with a central layer of expanded polyurethane (200 mm). In the central part of it there is an opening for the placement of the sample, with 0.30 × 0.30 m dimensions. The contact zones between the support panel and the sample are covered with insulation rubber in the perimeter joints, which are also sealed with silicone during the

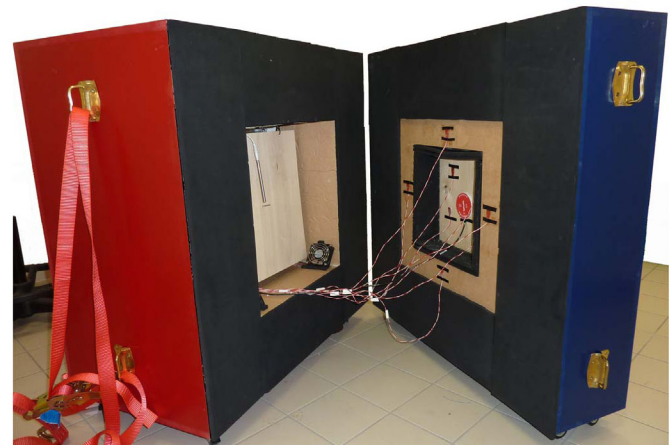


Fig. 2. General view of the apparatus Small Hot-Box.

test.

The cold side of the system is the laboratory room (internal dimensions 3.39 m × 4.22 m × 2.97 m high), completely insulated from the outside. The small Hot-Box is positioned inside this room, where it is not possible to set the temperature but it was monitored during a long period before the construction of the apparatus and it was observed that the daily temperatures are very steady (maximum difference about 0.8 °C). During the test, the temperatures inside the hot room are maintained constant by means of a heating source made of a 3 m long (50 W) S-shaped heating wire. In order to avoid direct radiation effects, a screen (baffle) made of poplar wood (emissivity 0.90) is placed between the heating system and the support panel. The heating wire is switch on and off automatically thanks to a PID (Proportional-Integral-Derivative) control system. Inside the hot chamber, 9 thermoresistances are installed in order to control the surface temperatures of the sample (4 probes), of the support panel (4 probes), and the air temperature (1 probe). In the laboratory cold side, 8 probes are fixed to the surface of the specimen and of the support panel, and one is placed in the room for air temperature measurement. Finally a thermal flux meter is placed in the central area of the sample, in order to measure the heat flux from the hot side to the cold one. The apparatus diagram with the sensors' position are represented in Fig. 3 [34]. All the monitored data are transferred to a PC: it is possible to select the time step for the data acquisition, and it is also possible to visualize and save the acquired data. In order to avoid the air stratification, two fans (each one with an electric current equal to 0.11 A) were installed inside. A convective equilibrium was achieved thanks to this ventilation system and a maximum difference of about 0.6 °C on the hot face was achieved after the fans' installation.

A switchboard was finally assembled: it is composed of a master switch, a PID controller, an electrical energy meter, and a

**Table 2**  
Description of the samples for thermal measurements.

Samples	Description	s <sub>plasterboard</sub> (mm)	s <sub>coating</sub> (mm)	s <sub>total</sub> (mm)
PL	Plasterboard sheet	13	–	13
D	Plasterboard+mortar with clay, cork and natural lime	13	42	55
R	Plasterboard+mortar with natural lime, limestone sand, aggregates	13	44	57
R2	Plasterboard+mortar with natural lime, limestone sand, aggregates	13	43	56
C	Plasterboard+mortar with cement, aggregates and other additives with high mechanical strength	13	43	56
D-FRP	Plasterboard+mortar with clay, cork and natural lime with Glass Fibre Reinforced grid	13	42	55
R-FRP	Plasterboard+mortar with natural lime, limestone sand, aggregates with Glass Fibre Reinforced grid	13	45	58
R2-FRP	Plasterboard+mortar with natural lime, limestone sand, aggregates with Glass Fibre Reinforced grid	13	42	55
C-FRP	Plasterboard+mortar with cement, aggregates and other additives with high mechanical strength with Glass Fibre Reinforced grid	13	44	57

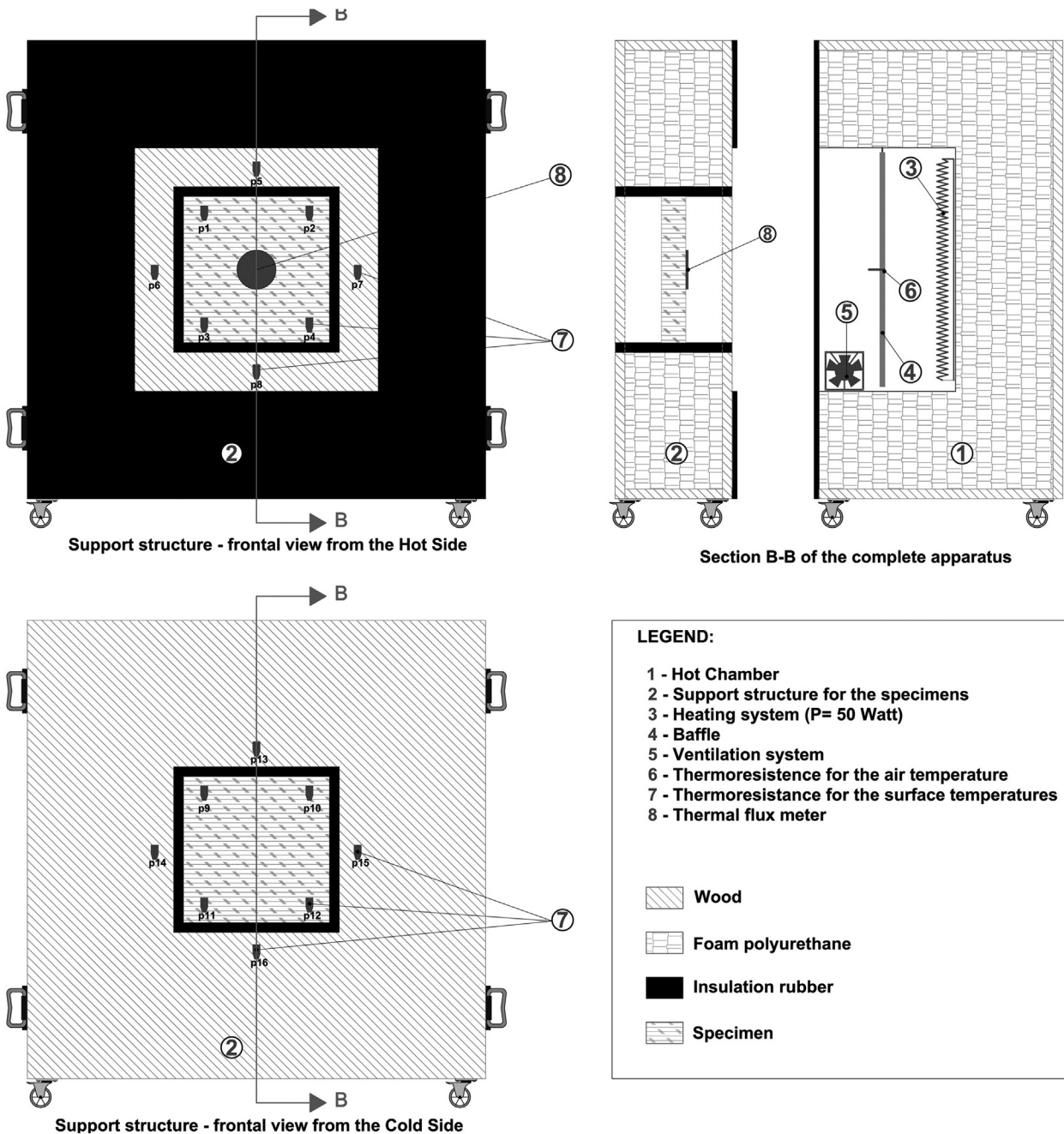


Fig. 3. Apparatus diagrams and sensors' positions.

speed variator for the regulation of the fans' velocity. Considering the evaluation of the heat flow supplied to the hot chamber in order to keep the steady-state conditions, an ammeter was also installed in order to evaluate the current passing through the hot wire. The heat power released by the resistance during a test could be evaluated as the product of the hot wire thermal resistance (measured in Ohm) and the square current through the hot wire (in ampere). On the contrary the electric energy meter measures directly the energy entering the hot side, but it has a low accuracy and it was used only as a control instrument.

The Hot Box method could be used for calculating the thermal conductivity of the samples, by evaluating the heat flux through the sample as the difference between the input power ( $P_i$  in W) in the hot chamber and the heat losses through the walls and the thermal bridges ( $P_w$  in W). The incoming power  $P_i$  can be measured considering two contributes: the heat flux released by the

resistance during the test ( $P_r$  in W) and the contribute of the fans ( $P_f$  in W). The contribution of the losses  $P_w$  is evaluated by means of calibration measurements and it shall be plotted vs. the air temperature difference between the hot and the cold side.

$$P_s = P_i - P_w \quad [W] \quad (1)$$

where:

- $P_s$  is the power coming out through the tested specimen (W);
- $P_i$  is the entering power in the hot chamber, measured by a power meter (W);
- $P_w$  is the power loss through the walls and the thermal bridges, evaluated by the calibration curve Eq. (6) (W).

The thermal conductivity of the specimen is then calculated by dividing the product of the power through the specimen ( $P_s$  in W)

and its thickness by the area of the specimen  $A_s$  ( $\text{m}^2$ ) and the surface temperature difference between its two sides:

$$\lambda = \frac{P_s \cdot s}{A_s \cdot (T_{SH} - T_{SC})} \quad [\text{W}/(\text{m K})] \quad (2)$$

Specific calibration panels (foam polyurethane, expanded polystyrene, plasterboard, and wood) were assembled for the calibration tests and many measurements were carried out by considering different set-point temperatures of the hot chamber (the air temperature difference between hot and cold side was maintained higher than  $20^\circ\text{C}$  for all the tests). Generally it was observed that the mean error of the apparatus decreases by decreasing the set point temperature of the hot side. A mean value of  $50^\circ\text{C}$  for the hot chamber was considered.

The thermal flux meter method is based on a thermal flux meter probe placed in the central part of the sample, as shown in Fig. 3. The probe (model HP01 – Hukuseflux) is a thermopile operating in the  $-2000 \div +2000 \text{ W/m}^2$  power range and in the  $-30 \div +70^\circ\text{C}$  temperature range. It measures the differential temperature across the ceramics-plastic composite body and generates a small output voltage proportional to the local heat flux. In order to calculate the thermal conductivity, 8 thermoresistances are installed on the surface of the sample, with four sensors each side (Fig. 3). The thermal resistance  $R_t$  could be calculated as follows (Progressive Average Methodology) [35,36]:

$$R_t = \frac{\sum_{j=1}^n (T_{SHj} - T_{SCj})}{\sum_{j=1}^n q_j} \quad [(\text{m}^2 \text{ K})/\text{W}] \quad (3)$$

where the index  $j$  is related to each acquisition time,  $T_{SHj}$  is the mean value of the panel surface temperature of the Hot side,  $T_{SCj}$  is the mean value of the panel surface temperature in the Cold side, and  $q$  is the heat flux through the sample ( $\text{W/m}^2$ ). The average values of the temperatures of the four sensors installed in each side of the sample and the mean thermal heat flux were used for the calculation.

The value of the thermal conductivity can be calculated by the mean value of the thermal resistance  $R_t$  during the selected period (about 2–3 h) and the thickness of the specimen ( $s$  in m):

$$\lambda = s/R_t \quad [\text{W}/(\text{m K})] \quad (4)$$

### 2.3. Mechanical characterization

The strengthening technique is very similar of the traditional steel jacketing for masonry wall panels. Both G-FRP and thermal insulating mortars underwent a mechanical characterization. The mechanical properties of the mortars were evaluated by compression tests in compliance with EN 12390-2 2009 [37]. Compressive strength of mortar at 30 days after casting has been measured.

In order to study the shear behaviour of the wall panels reinforced with thermal insulating plaster, 10 wall panels were tested in diagonal tension [38,39], as reported in Fig. 4.

Using the Turnšek and Cacovic [40] formulation, the shear strength is:

$$\tau = \frac{f_t}{1.5} = \frac{p}{3 \cdot A_n} \quad (5)$$

in which  $p$  is the diagonal load and  $A_n$  is the cross-section area of the wall panel. For both unreinforced and reinforced wall panels, brickwork pattern was made from all headers (*header bond pattern*) on each course. Panels were assembled by using a lime-based mortar for construction in laboratory.

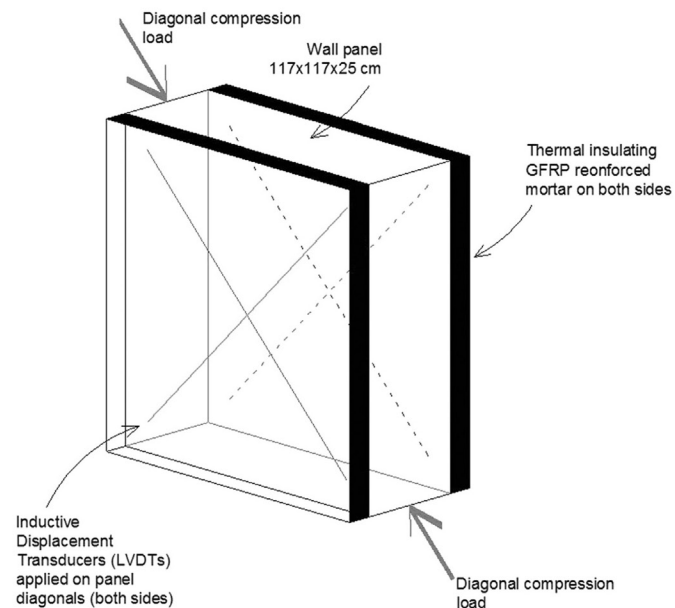


Fig. 4. Test set-up for mechanical characterization.

## 3. Results

### 3.1. Thermal properties

By applying the Hot-Box method data was calculated with a calibration curve based on materials with a known thermal conductivity higher than  $0.06 \text{ W/mK}$  (for the calibration curve construction a wood panel ( $\lambda=0.12 \text{ W/mK}$ ), a plasterboard panel ( $\lambda=0.20 \text{ W/mK}$ ) and an insulating panel with wood fibres and cement ( $\lambda=0.065 \text{ W/mK}$ ) were used). The following calibration curve was used:

$$P_W = 0.2487 \cdot \Delta T_a + 1.4567 \quad [\text{W}] \quad (6)$$

where:

- $P_W$  is the power loss through the walls and the thermal bridges ( $\text{W}$ );
- $\Delta T_a$  is the air temperature difference between the hot and the cold side ( $^\circ\text{C}$ ).

By measuring  $P_i$  in Eq. (1),  $P_s$  and  $\lambda$  of the sample could be calculated by applying Eqs. (1) and (2).  $\lambda$  of the coating should then be calculated knowing  $\lambda$  and  $s$  of the plasterboard panel used as support base, by applying the following:

$$\lambda_{coating} = \frac{s_{coating}}{\frac{s_{total}}{\lambda_{total}} - \frac{s_{plasterboard}}{\lambda_{plasterboard}}} \quad [\text{W}/(\text{m K})] \quad (7)$$

Results are showed in Table 3.

It can be observed that the R-FRP and R2-FRP have the best thermal insulation behaviour, while the C type has the highest thermal conductivity ( $0.275 \text{ W/mK}$  without G-FRP and  $0.189 \text{ W/mK}$  with G-FRP grid). The same data was obtained by using the thermal flux meter methodology. The thermal conductivity of the plasterboard is  $0.19 \text{ W/mK}$  (with a difference of only 5% in respect to the value declared from the company, equal to  $0.2 \text{ W/mK}$ ).

Table 4 shows the thermal conductivity values obtained for the different specimens, with and without reinforced grid system: the comparison between the results is represented in the table considering both the methodologies.

All the coatings have good thermal properties, even if they

**Table 3**

Thermal conductivity values with Hot-Box method.

Samples	$\Delta T_a$ (°C)	$P_i$ (W)	$P_w$ (W)	$P_s$ (W)	s (m)	Thermal conductivity of the mortar (HB method) (W/mK)
D	23.95	11.78	7.41	4.37	0.042	<b>0.123</b>
R	27.17	11.04	8.21	2.83	0.044	<b>0.074</b>
R2	24.58	11.71	7.57	4.14	0.043	<b>0.130</b>
C	23.42	12.91	7.28	5.63	0.043	<b>0.275</b>
D-FRP	22.86	10.22	7.14	3.08	0.042	<b>0.107</b>
R-FRP	20.29	9.35	6.50	2.85	0.045	<b>0.105</b>
R2-FRP	27.56	12.14	8.31	3.83	0.042	<b>0.101</b>
C-FRP	22.03	10.77	6.94	3.83	0.044	<b>0.189</b>

were developed as structural mortars; generally the thermal conductivities are lower than the ones of traditional coatings (values in 0.5–1.0 W/mK range).

The thermal conductivity values of the samples with G-FRP vary between 0.089 and 0.210 W/mK. The best mortar is R2-FRP type, the worst is C-FRP (0.210 W/mK), but it is the best coating considering the mechanical resistance of the samples (see paragraph 3.2). The thermal conductivity of the samples with G-FRP decreases of about 11–15% with respect to samples without G-FRP, except for R: in this case it is possible to observe an increasing of about 8% probably due to a flaw of the mortar grout during the laying of the samples (Fig. 5); the improvement in terms of reduction of the thermal conductivity (about 11–15%) is probably due to air included in the mixture.

Furthermore it is important to observe that the thermal conductivities of the samples with and without G-FRP are not so different from the error value of the apparatus (about 10%), and therefore they are not so different in terms of thermal performance: minimum changes of the final thermal conductivity values are attributed especially to differences in the laying of the samples.

Considering the comparison between the two methodologies (Hot Box and Thermal Flux Meter, see Table 4) it can be observed that the differences vary in 9–23% range: the thermal conductivities obtained with the Hot-Box Method are in general higher than the ones obtained by the Thermal Flux Meter Method for almost all the samples. Nevertheless the Thermal Flux Meter Method seems more reliable, because the considered calibration curve used for the Hot-Box method is preliminary and much more materials with  $\lambda$  in 0.05–0.50 W/(mK) range should be used for the improvement of that curve (6).

### 3.2. Mechanical resistance

The technical developments of the last years have enabled to produce new mortars with specific properties, such as a low salt content and size of the aggregate in function of the masonry characteristics in order to achieve the highest possible

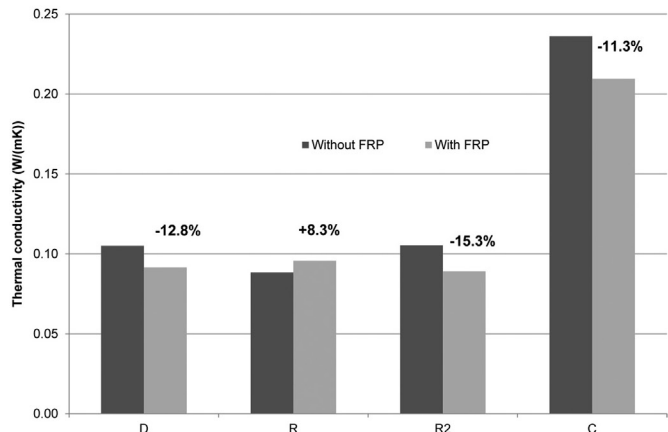


Fig. 5. Thermal flux meter method: thermal conductivity differences between mortars with and without G-FRP.

compatibility with existing masonry. Sixteen 94 mm diameter cylindrical samples (four for each mortar type) have been tested for compression. Mortar cylinders were approx. 180 mm in height. The average compression strength of the cylindrical samples at 30 days after casting was 0.66, 0.72, 0.87, and 2.70 MPa respectively for mortars D-, R-, R2-, and C-type (Table 5). These values are similar both in terms of compressive strength and Young's modulus with the mortar's mechanical properties of historic stone multi-leaf masonry walls [41].

#### 3.2.1. Un-reinforced panels

When subjected to shear tests in diagonal tension, all un-reinforced panels exhibited a failure along the compressed panel diagonal. If the diagonal compression force is strong enough to exceed the lateral strength capacity of the wall panel, diagonal cracking opened slowly in the mortar joints and in the bricks starting from the central part of the wall panel and producing a tensile failure of the walls and an abrupt loss of lateral stiffness (shear modulus). Two unreinforced brickwork panels have been tested (test n. 5 and 6) and the average lateral capacity and shear strength  $\tau$  were respectively 201.1kN and 0.230 MPa, while the shear modulus  $G$  was 4078 MPa. Results are summarized in Table 6.

#### 3.2.2. Reinforced panels

Eight reinforced masonry panels were subjected to the diagonal tension test and a single test was performed on each wall panel. In-plane resistance of unreinforced masonry wall panels is mainly based on the thermal insulating mortar strength. Table 6 gives the results in terms of diagonal compression capacity, shear strength and modulus for each test.

For panels reinforced with D-type mortar, as expected, the wall

**Table 4**

Thermal conductivity values with thermal flux meter method and comparison with the Hot-Box method.

Samples	$T_{aH}$ (°C)	$T_{ac}$ (°C)	$\Delta T_a$ (°C)	$\Delta T_s$ (°C)	Heat flow through the sample (W/m <sup>2</sup> )	Total thermal resistance $R_t$ (m <sup>2</sup> K/W)	Thermal conductivity of the mortar (tfm method) (W/mK)	Thermal conductivity of the mortar (HB method) (W/mK)	Differences between tfm and HB methods (%)
Plasterboard	50.22	23.14	27.08	14.80	68.61	0.216	<b>0.190</b>	—	—
D	45.32	21.37	23.95	16.56	41.44	0.400	<b>0.105</b>	<b>0.123</b>	<b>17.1</b>
R	50.36	23.19	27.17	20.72	36.56	0.567	<b>0.088</b>	<b>0.074</b>	<b>15.9</b>
R2	45.33	20.75	24.58	18.25	38.28	0.477	<b>0.105</b>	<b>0.130</b>	<b>23.7</b>
C	45.30	21.88	23.42	13.86	55.34	0.250	<b>0.236</b>	<b>0.275</b>	<b>16.5</b>
D-FRP	45.38	22.52	22.86	15.64	34.11	0.459	<b>0.092</b>	<b>0.107</b>	<b>16.3</b>
R-FRP	45.49	25.20	20.29	15.56	28.87	0.539	<b>0.096</b>	<b>0.105</b>	<b>9.3</b>
R2-FRP	50.35	22.79	27.56	20.52	38.81	0.540	<b>0.089</b>	<b>0.101</b>	<b>13.4</b>
C-FRP	45.35	23.32	22.03	12.68	45.54	0.278	<b>0.210</b>	<b>0.189</b>	<b>10.0</b>

**Table 5**

Mechanical properties of thermal insulating mortars.

Mortar denomination	Sample size	Compression strength (MPa)	Bending strength (MPa)	Young modulus (MPa)
D	4	0.66	0.14	580
R	4	0.72	0.13	1130
R2	4	0.87	0.23	1030
C	4	2.70	0.43	2396

**Table 6**

Results of mechanical testing.

Test N.	Maximum diagonal load $p$ (kN)	Shear strength (MPa)	Shear strength increment (%)	Shear Modulus $G$ (MPa)
1_R-FRP	202.86	0.232*	0.8	4247
2_R-FRP	228.30	0.261*	13.5	5412
3_D-FRP	236.47	0.271*	17.6	3981
4_D-FRP	258.50	0.296*	28.5	4127
5_R	204.50	0.234	–	4466
6_R	197.73	0.226	–	3691
7_R2-FRP	315.59	0.361*	56.9	3528
8_R2-FRP	325.49	0.373*	62.2	–
9_C-FRP	431.41	0.494*	114.8	3431
10_C-FRP	420.33	0.481*	109.1	–

\* Calculated using 250 mm panel thickness.

panels reinforced with this technique did not result very stiff (shear modulus  $G=4054$  MPa). Lateral capacity was 247.5 kN. The stress-strain curve shows a quasi-elastic behaviour with a weak yield plateau. The failure mode involved a sudden loss of collaboration between the reinforcement (lime mortar) and substrate (masonry), with some cracks along the compressed diagonal observed on mortar surface.

The results of the shear tests did not show a significant high increases both in terms of shear strength and stiffness when mortar type R has been applied. The lateral capacity and stiffness (shear modulus) values became, respectively, 215.6 kN and 4829 MPa, with a limited increment of 7% and 18.4% when compared to the values measured for the same panels before reinforcement. The failure modes observed for these panels are characterized by a very similar cracking pattern as those of the unreinforced (Fig. 6).

For wall panels reinforced using thermal insulating mortars R2 and C-type, a significant enhancement of the shear strength was



Fig. 6. Reinforced panel after failure.

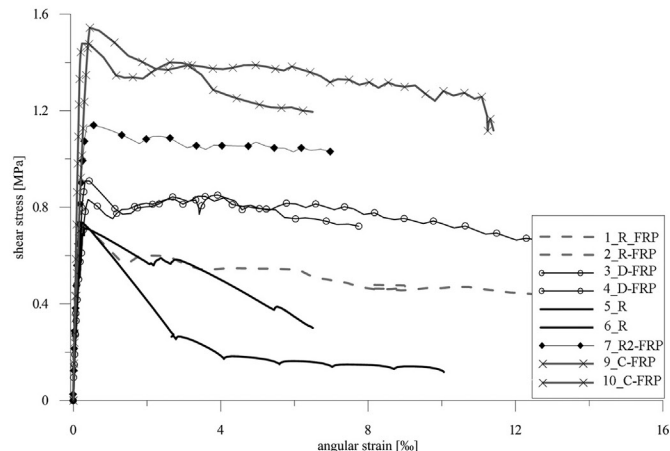


Fig. 7. Elastic and plastic behaviour of the reinforced and un-reinforced panels.

detected: an increase of 114.8% and 109.1% was measured for R2 and C-type mortar, respectively.

From these test results, a clear tendency is evident: the reinforcing technique can cause an increase of the shear stiffness only if a thermal insulating mortar with good mechanical properties is used (type R2 or C). For reinforced panels shear stress versus angular strain responses, such as those shown in Fig. 7, a two-stage behaviour has been detected: for small values of the angular strain (approx. up 0.5%) the behaviour is almost linear elastic while it becomes highly inelastic for larger values of the deformation. The elastic phase of the reinforced panels curves is characterized by a similar slope as those of the un-reinforced. Thus, a first consequence of the reinforcement is the increase of the strength of the wall while leaving unchanged the in-plane stiffness measured in the elastic phase.

#### 4. Conclusions

The present paper is focused on the importance of combining thermal and mechanical properties in buildings refurbishment. The use of construction materials with good thermal properties is in fact the first condition for greatly reducing the thermal heat losses of the final products. The study is focused on glass fibre reinforced insulating mortars: they combine good mechanical and thermal properties for building refurbishment.

The insulating behaviour of the coatings was investigated by an original experimental apparatus named Small Hot-Box. It is an effective alternative system used instead of the Hot-Plate apparatus for the experimental evaluation of the thermal resistance of homogeneous materials. The tested samples are installed in a support panel between the hot and the cold sides; an air temperature difference is maintained during the test. A heat flux passes through the sample during the test: the thermal conductivity can be evaluated by measuring the heat flux and the surface temperatures of the specimen. Two different methodologies are presented: the thermal flux meter method and the Hot-Box one. The first method takes into account the heat flux measured by the thermal flux meter installed on the sample, the second one evaluates the heat flux through the specimen as the difference between the input heat flux and the heat losses through the walls.

Considering the thermal flux meter method, all the coatings have good thermal properties (thermal conductivities variable in 0.09–0.23 W/(mK) range) and the best thermal behaviour can be attributed to R and R2 mortars. Also considering the Hot-Box method, the lowest thermal conductivities were found for R and R2 mortars. Results obtained by considering the two

methodologies are aligned, nevertheless the thermal flux meter method results should be considered more reliable because the calibration curve used for the Hot-Box method is just preliminary and it should be improved. The best thermal performance were obtained for the samples D, R, and R2 ( $\lambda=0.09\text{--}0.105\text{ W/mK}$ ), while for C a value of  $0.19\text{--}0.27\text{ W/mK}$  was found.

Generally, with the glass fibre reinforced grid the thermal conductivity of the samples decreases of about 11–15% except for mortar type R but this behaviour is probably due to the small dimensions of the specimens; anyway it is expected that the thermal resistance of the mortars *in situ* would not significantly modified by the G-FRP insertion.

The externally applied G-FRP mesh to masonry panels resulted in a stronger system, as compared to the un-reinforced configuration. The addition of a G-FRP reinforced coating resulted in an increase in-plane load capacity between 7% and 115%. However the reinforcement can produce an increase of the in-plane load-capacity only if a thermal insulating mortar with good mechanical properties is used; large increases in shear capacity were only found for wall panels reinforced with thermal mortars R2 and C: it demonstrates that the G-FRP grid upgrade with a lime-based thermal insulating mortar is promising, but less effective compared to the reinforcement with epoxy resins or concrete coatings. Mechanical shear tests have demonstrated that the adhesion between the masonry panels and the coating used as a base for reinforcement (G-FRP mesh) was the critical element in the reinforcing system. Failure of reinforced panels resulted from the separation of the layer of thermal insulating mortar from the masonry panels and from the opening of diagonal cracks along the compressed panel's diagonal.

Finally, by combining results of thermal and mechanical characterization, the samples with the R2 mortar seem the more promising for building refurbishment, being the best compromise between thermal and mechanical performance.

## References

- [1] European Commission, Energy-Efficient Buildings PPP – Multi-Annual Roadmap and Longer Term Strategy, Available at: [\(\[http://ec.europa.eu/information\\\_society/activities/sustainable\\\_growth/docs/sb\\\_publications/eeb\\\_roadmap.pdf\]\(http://ec.europa.eu/information\_society/activities/sustainable\_growth/docs/sb\_publications/eeb\_roadmap.pdf\)\)](http://ec.europa.eu/information_society/activities/sustainable_growth/docs/sb_publications/eeb_roadmap.pdf) (last access 14.11.14).
- [2] C. Buratti, E. Belloni, D. Palladino, Evolutive Housing system: refurbishment with new technologies and unsteady simulations of energy performance, *Energy Build.* 74 (2014) 173–181.
- [3] L. Pérez-Lombard, J. Ortiz, C. Pout, A review on buildings energy consumption information, *Energy Build.* 40 (3) (2008) 394–398.
- [4] BPIE (Building Performance Institute Europe), Europe's Buildings Under the Microscope 2011, Available at: [\(\[http://www.bpie.eu/eu\\\_buildings\\\_under\\\_microscope.html\]\(http://www.bpie.eu/eu\_buildings\_under\_microscope.html\)\)](http://www.bpie.eu/eu_buildings_under_microscope.html) (last access 14.11.14).
- [5] Directive 2010/31/EU of the European Parliament and of the Council of 19 May 2010 on the Energy Performance of Buildings (recast).
- [6] American Society for Testing and Materials, ASTM C177-97: Standard Test Method for Steady-State Heat Flux Measurements and Thermal Transmission Properties by Means of the Guarded-Hot-Plate Apparatus, West Conshohocken, PA, 1997.
- [7] S. André, B. Rémy, F. Pereira, N. Cella, Hot wire method for the thermal characterization of materials: inverse problem application, *Eng. Térmica* 4 (2003) 55–64.
- [8] Y. Jannot, V. Felix, A. Degiovanni, A centered hot plate method for measurement of thermal properties of thin insulating materials, *Meas. Sci. Technol.* 21 (3) (2010) 1–8.
- [9] Y. Jannot, B. Rémy, A. Degiovanni, Measurement of thermal conductivity and thermal resistance with a tiny hot plate, *High Temp. High Press.* 39 (2009) 11–31.
- [10] N. Laaroussi, G. Lauriat, M. Garoum, A. Cherki, Y. Jannot, Measurement of thermal properties of brick materials based on clay mixtures, *Constr. Build. Mater.* 70 (2014) 351–361.
- [11] J.R. Mumaw, Calibrated hot box: an effective means for measuring thermal conductance in large wall sections. In: American Society for Testing and Materials, ASTM STP 544, Heat Transmission Measurements in Thermal Insulations, West Conshohocken, PA, 1974, pp. 193–211.
- [12] J.H. Klem, A calibrated hot box for testing window systems – Construction calibration and measurements on prototype high-performance windows, In: Proceedings of ASHRAE/DOE-ORNL Conference on Thermal Performance of the Exterior Envelopes of Buildings, Kissimmee, Florida, 1979, pp. 338–346.
- [13] European Standard EN ISO 8990, Thermal Insulation – Determination of Steady-state Thermal Transmission Properties – Calibrated and Guarded Hot Box, 1996.
- [14] European Standard EN ISO 12567-1, Thermal Performance of Windows and Doors – Determination of Thermal Transmittance by Hot Box Method – Complete Windows and Doors, 2010.
- [15] UNI EN 1934, Prestazione termica degli edifici – Determinazione della resistenza termica per mezzo del metodo della camera calda con termoflussimetro – Muratura, 2000 (in Italian).
- [16] F. Asdrubali, G. Baldinelli, Thermal transmittance measurements with the hot box method: Calibration, experimental procedures, and uncertainty analyses of three different approaches, *Energy Build.* 43 (2011) 1618–1626.
- [17] C. Fangzhi, K.W. Stephen, Summer condition thermal transmittance measurement of fenestration systems using calorimetric hot box, *Energy Build.* 53 (2012) 47–56.
- [18] A.H. Elmahdy, K. Haddad, Experimental procedure and uncertainty analysis of a guarded hot box method to determine the thermal transmission coefficient of skylights and sloped glazing, *ASHRAE Trans.* 106 (2) (2000) 601–613.
- [19] K. Martin, A. Campos-Celador, C. Escudero, I. Gómez, J.M. Sala, Analysis of a thermal bridge in a guarded hot box testing facility, *Energy Build.* 50 (2012) 139–149.
- [20] P. Ricciardi, E. Belloni, F. Cotana, Innovative panels with recycled materials: thermal and acoustic performance and life cycle assessment, *Appl. Energy* 134 (2014) 150–162.
- [21] European Standard EN ISO 12667, Thermal Performance of Building Materials and Products-Determination of Thermal Resistance by Means of Guarded Hot Plate and Heat Flow Meter Methods-Products of High and Medium Thermal Resistance, ISO, Geneva, Switzerland, 2001.
- [22] American Society for Testing and Materials, ASTM C518-10. Standard Test Method for Steady-State Thermal Transmission Properties by Means of the Heat Flow Meter Apparatus, ASTM, West Conshohocken, PA, USA, 2003.
- [23] S.W. Kim, S.H. Lee, J.S. Kang, K.H. Kang, Thermal conductivity of thermoplastics reinforced with natural fibres, *Int. J. Thermophys.* 27 (2006) 1873–1881.
- [24] M.R. Ehsani, H. Saadatmanesh, J.I. Velazquez-Dimas, Behavior of retrofitted URM walls under simulated earthquake loading, *J. Compos. Constr.* 3 (3) (1999) 134–142.
- [25] A. Borri, M. Corradi, A. Vignoli, New Materials for Strengthening and Seismic Upgrading Interventions, International Workshop Ariadne, vol. 10, 2002, pp. 22–28.
- [26] M. Corradi, A. Borri, A. Vignoli, Experimental evaluation of the in-plane shear behaviour of masonry walls retrofitted using conventional and innovative methods, *J. Br. Mason. Soc.* 21 (1) (2008) 29–42.
- [27] M.R. Valluzzi, D. Tinazzi, C. Modena, Shear behavior of masonry panels strengthened by FRP laminates, *Constr. Build. Mater.* 16 (2002) 409–416.
- [28] C.G. Papanicolaou, T.C. Triantafyllou, M. Papathanasiou, K. Karlos, Textile Reinforced Mortar (TRM) versus FRP as strengthening material of URM walls: out-of-plane cyclic loading, *Mater. Struct.* 41 (2008) 143–157.
- [29] M. Corradi, A. Borri, G. Castori, R. Sisti, Shear strengthening of wall panels through jacketing with cement mortar reinforced by GFRP grids, *Compos. Part B: Eng.* 64 (2014) 33–42.
- [30] A. Enfedaque, J.C. Gálvez, F. Suárez, Analysis of fracture tests of glass fibre reinforced cement (GRC) using digital image correlation, *Constr. Build. Mater.* 75 (2015) 472–487.
- [31] C. Buratti, E. Moretti, E. Belloni, F. Agosti, Development of innovative aerogel based plasters: preliminary thermal and acoustic performance evaluation, *Sustainability* 6 (2014) 5839–5852.
- [32] A. Borri, C. Buratti, M. Corradi, R. Sisti, G. Castori, E. Belloni, D. Palladino, Rinforzo a taglio di pannelli murari con intonaci termoisolanti fibrorinforzati. III Convegno di Ingegneria Forense. VI Convegno su Crolli, Affidabilità Strutturale, Consolidamento. Sapienza Università di Roma, 14–16 Maggio 2015 (In Italian).
- [33] A. Borri, M. Corradi, R. Sisti, C. Buratti, E. Belloni, E. Moretti, Masonry wall panels retrofitted with thermal-insulating GFRP-reinforced jacketing, *Mater. Struct.* (2015), [\(<http://dx.doi.org/10.1617/s11527-015-0766-4>\)](http://dx.doi.org/10.1617/s11527-015-0766-4).
- [34] C. Buratti, E. Belloni, L. Lunghi, M. Barbanera, Thermal conductivity measurements by means of a new 'small hot-box' apparatus: manufacturing, calibration and preliminary experimental tests on different materials, *Int. J. Thermophys.* (2016) 37–47, [\(<http://dx.doi.org/10.1007/s10765-016-2052-2>\)](http://dx.doi.org/10.1007/s10765-016-2052-2).
- [35] prEN 12494, Building Components and Elements – In Situ Measurement of the Surface Thermal Resistance, 1996.
- [36] C. Buratti, S. Grignaffini, Measurement of the thermal resistance of masonry walls, *Int. J. Heat Technol.* 21 (2) (2003) 107–114.
- [37] EN 12390-2, Testing Hardened Concrete – Part 2: Making and Curing Specimens for Strength Tests, 2009.
- [38] ASTM E519, Standard Test Method for Diagonal Tension Shear in Masonry Assemblages, 2002.
- [39] RILEM TC, 76-LUM. Diagonal tensile strength tests of small wall specimens, 1991, in: RILEM (Ed.), RILEM Recommendations for the Testing and Use of Construction Materials. E & FN SPON, London, 1994, pp. 488–489.
- [40] V. Turnšek, F. Čačovič, Some experimental results on the strength of brick masonry walls, In: Proceedings of the 2nd International Brick Masonry Conference, Stoke-on-trent, 1970, pp. 149–156.
- [41] F. Da Porto, M.R. Valluzzi, C. Modena, Investigations for the knowledge of multi-leaf stone masonry walls, in: Proceedings of the 1st Int. Congr. on Construction History, Madrid, 20–24 January, 2003.